Infinite-order cumulant expansion for spins*

Michele Parrinello
Istituto di Fisica, Università di Messina, Messina, Italy
and Gruppo Nazionale di Struttura della Materia del Consiglio, Nazionale delle Ricerche, Messina, Italy

Tadashi Arai
Argonne National Laboratory, Argonne, Illinois 60439
(Received 7 February 1974)

The cumulant expansion for spins developed previously is rearranged and extended up to an infinite order in perturbation. A pair of spin-deviation lines is considered as a propagator and, as an additional propagator appears and interacts with the original one, that part of the diagram is defined as a self-energy correction. All cumulant corrections are decomposed and added to the corresponding self-energy corrections, so that self-energy corrections and their cumulant corrections are automatically calculated together exactly. The contribution of a self-energy correction to a diagram depends on the geometry of the incoming and outgoing spin-deviation lines of the self-energy diagram, yielding a new type of perturbation expansion. Numerical results suggest that the nature of the spin-spin correlation in the spin-1/2 case is distinct from that in other cases and that spins behave like fermions rather than bosons in this limit.

I. INTRODUCTION

Recent developments in neutron diffraction techniques are providing much detailed information on magnetic structure of a variety of materials. For instance, a new experiment on the spiral spin structure of Ho (Ref. 1) not only demonstrates a bunching of the magnetic moments along the easy axes of the hexagonal plane, but also suggests considerable modulations of the moments, making them larger along the easy directions than along the hard directions. Such modulations may be explained only if zero-point fluctuations of the moments are larger along the hard axes than along the easy axes. Although magnetic structures have been determined mostly classically, more precise experiments are revealing quantum deviations in many of them[2] and a more precise theory is needed to calculate them.

A simple spin-wave theory[3] predicts the temperature dependence of magnetization with remarkable accuracy, but it tends to overestimate zero-point deviations of the moments.[4] Exceptions are the large zero-point deviations observed in the quadratic-layer antiferromagnets K_2NiF_4, K_2MnF_4, and Rb_2MnF_4, in good agreement with the values predicted by spin-wave theory including the anisotropy. However, it is not really clear why the good agreement with spin-wave theory can be expected for the zero-point deviations; the thermal variation of magnetization depends on spin waves in the long-wavelength limit and hence may be predicted accurately by a simple spin-wave theory, whereas zero-point deviations of magnetic moments involve the spectrum more impartially and consequently depend also on the short-wavelength region, where the accuracy of the spin-wave approximation is questionable.

It is therefore desirable to calculate the ground state of an antiferromagnetic or spiral spin structure directly by perturbation expansions. The difficulty involved in such an approach is that spins, being neither bosons nor fermions, have complicated commutation relations. Consequently, usual many-body perturbation technique based on Wick's theorem cannot be applied to spins immediately.

To avoid this difficulty, one might expand spin operators in terms of boson operators, but the method becomes similar to the spin-wave theory and inherits its poor convergence, as is demonstrated in Davis's calculation.[5] It is also difficult to extend the calculation to higher orders owing to the appearance of the kinematical interaction,[6] which is just a reflection of the complicated commutation relations among the original spin operators. In the limit of spin-$\frac{1}{2}$, Stinchcombe *et al.*[7] were able to use spin operators directly in the calculation of ferromagnetic spin waves, but the entire exchange Hamiltonian including the z component is regarded as a perturbation. Hence it has the same drawback as Davis's approach and the results have to be renormalized by summing over all three diagrams (the contributions from the z component).

It seems more natural and efficient to regard spin operators S^+ and S^- as creation and destruction operators and generate Wick's theorem appropriate to these operators. The kinematical interaction is then automatically taken into account at each stage of a perturbation expansion and hence the convergence is expected to be better than any other method developed so far. In fact, Wick's theorem has been generalized in this manner,[8,9] and by applying it in Kubo's cumulant rearrangement of perturbation theory,[10] compact prescriptions for the calculation

of the antiferromagnetic ground state have been obtained.[9]

The prescriptions are so compact that we could program them into a computer to generate and calculate all possible diagrams necessary for the perturbation expansion up to the sixth order.[11] For three-dimensional lattices, the finite-order perturbation series appear to converge, but a more careful inspection of the calculation reveals that many cancellations are involved among distinct diagrams in the sixth order, casting some uncertainty on the accuracy of the results. As the dimensionality decreases the convergence becomes poorer and, in a linear chain, the contributions of the sixth-order perturbation become nearly comparable to those of the fourth order. In the case of a linear chain with spin-$\frac{1}{2}$, the calculated value of the zero-point deviation is, in fact, greater than $\frac{1}{2}$ and hence unphysical.

This suggests that it is necessary to extend the perturbation up to an infinite order before zero-point deviations of spins can be compared with experimental results. Since an infinite-order perturbation expansion has never been developed for spins, and it is not obvious how such a summation can be performed in practice, it is essential to establish the concept of self-energy corrections for spins. Since spins are interacting even in the unperturbed state, the definition of a self-energy correction is not trivial nor simple as will be discussed in Secs. IV and V. In this paper, a pair of spin-deviation lines is regarded as a propagator, and as an additional propagator appears and interacts with the original one; that part of the diagram is defined as a self-energy correction. As will be found in Sec. V, the contribution of a self-energy correction to a diagram depends on the geometry of the incoming and outgoing propagators of the self-energy diagram, complicating the summation. Cumulant corrections are decomposed into parts and divided into the corresponding self-energy corrections so that self-energy corrections and their cumulant corrections are automatically calculated together exactly. The decomposition of cumulants will be discussed in Sec. III, while the cumulant expansion developed previously will be reviewed in Sec. II. As far as we are aware, this is the first attempt to extend a cumulant expansion up to an infinite order.[12] The present method is developed as if it is applied to an antiferromagnetic ground state, but it can be generalized for the calculation of spin-wave spectra, including the kinematical interaction, exactly. For this purpose alone, however, more precise information on the ground state is needed. The numerical results in Sec. VI will not only provide useful information as to what types of diagrams should be included in a particular problem, but also suggest that the nature of the spin-spin correlation in the spin-$\frac{1}{2}$ case is distinct from that in other cases and spins behave like fermions rather than bosons in this limit.

II. SUMMARY OF THE CUMULANT PERTURBATION EXPANSION

Let us consider the two-sublattice structure such that the nearest neighbors of an atom, say a, on sublattice A are on sublattice B and vice versa. Let S_a and S_b be spin operators of atoms of types a and b, respectively, and assume that the values of spins S_a and S_b are all equal, $|S_a| = |S_b| = j$. The anisotropic exchange Hamiltonian may then be written as

$$H = H_0 + \lambda H_I \quad , \tag{2.1a}$$

$$H_0 = -2J\sum_{(ab)} S_a^z S_b^z \quad , \tag{2.1b}$$

$$H_I = (1-\gamma) J \sum_{(ab)} (S_a^+ S_b^+ + S_a^- S_b^-) \quad , \tag{2.1c}$$

where $J>0$, the summation $\sum_{(ab)}$ runs over all the pairs of nearest neighbors, and $(1-\gamma)$ is the anisotropy parameter. For convenience, the alternating coordinates are used so that the z axes are always along the direction of the sublattice magnetization.

The ground state of H_0,

$$|0\rangle = |-j, -j, \ldots, -j\rangle \quad , \tag{2.2}$$

may be considered as the vacuum state, since

$$S_a^-|0\rangle = S_b^-|0\rangle = 0 \quad . \tag{2.3}$$

The energy of the system is then given by

$$E = E_0 + \sum_{n=0}^{\infty} \langle 0| H_I \left(\frac{1}{E_0 - H_0} H_I\right)^n |0\rangle_{\text{cum}} \quad , \tag{2.4}$$

and our problem is reduced to the calculation of cumulant matrix elements $\langle 0| \cdots |0\rangle_{\text{cum}}$.

Since nth-order terms contain n pairs of spin deviations $S_a^+ S_b^+$ or $S_a^- S_b^-$, which are connected with each other through the interaction $(1-\gamma)J$ and distributed among atoms in a cluster, they may be computed as follows.

(i) Construct all possible and topologically distinct atomic clusters containing at least two atoms but not more than n atoms. All atoms in a cluster must be connected with each other through the interaction J involved.

(ii) Distribute $\frac{1}{2}n$ pair creations $S_a^+ S_b^+$ and $\frac{1}{2}n$ pair destructions $S_a^- S_b^-$ in all possible time sequences and in all possible ways among atoms in the cluster. This process may be described by diagrams as follows. As time increases to the left, S^+ and S^- will be denoted by right (○) and left (×) terminals, respectively, of horizontal line segments showing the propagation in time of a spin deviation on an atom. For each atom involved, draw a different

line and, whenever possible, neighboring atoms will be shown on neighboring lines. A pair creation $S_a^+S_b^+$ or pair destruction $S_a^-S_b^-$ on neighboring atoms is denoted by a zig-zag line connecting the corresponding two terminals. This divides the diagram into $n-1$ time intervals.

(iii) Draw all possible contractions of spin deviations involved in a diagram. Overlapping spin deviations yield more than one set of contractions. This would divide a diagram into one or more subclusters, where a subcluster is an ensemble of terminals connected to each other by contraction lines and zig-zag (pair-creation or -destruction) lines.

Let us denote by $\langle A_m \cdots A_2A_1\rangle_{\text{cum}}$ the value of the diagram consisting of m subclusters $A_1A_2\cdots A_m$ and including the cumulant corrections. Then

$$\langle A_m \cdots A_2A_1\rangle_{\text{cum}} = \sum_{l=1}^{m} \sum_{\substack{\text{all possible}\\ l \text{ partitions}}} (-1)^{l-1}(l-1)! \times \langle A_{i_1}\cdots\rangle \langle A_{i_2}\cdots\rangle \cdots \langle A_{i_l}\cdots\rangle, \tag{2.5}$$

where $A_{i_1}\cdots$, $A_{i_2}\cdots$, $\ldots$, $A_{i_l}\cdots$, illustrate one way to divide m variables $A_m\cdots A_2A_1$ into l parts. $\langle A_{i_1}\cdots\rangle$ is the value of the small diagram consisting of subclusters $A_{i_1}\cdots$ and not including the cumulant corrections. The calculation of diagrams may then proceed as follows.

(iv) For the numerical value of a diagram before cumulant corrections, (a) for each time interval, multiply by the inverse of the value of

$$E_0 - H_0 = -(4zjp - 2q)J \ , \tag{2.6}$$

where z is the coordination number, $2p$ is the number of spin deviations, and q is the number of interactions among the spin deviations which exist during that time interval; (b) for each contraction with time interval t, multiply by a factor $2(j-n)$, where n is the number of contractions for the same atom covering the entire interval t.

(v) For the cumulant corrections for a diagram with more than one subcluster, form all distinct partitions of the diagram into subdiagrams composed of one or more subclusters. For each partition repeat steps (iv a) and (iv b), by regarding them as if the subdiagrams are spatially separated from one another. Multiply by the factor $(-1)^{l-1}(l-1)!$ involved in Eq. (2.5), sum over all partitions, and add to (iv). This yields the value of $\langle A_m\cdots A_2A_1\rangle_{\text{cum}}$.

(vi) For each diagram, multiply the value of $\langle A_m\cdots A_2A_1\rangle_{\text{cum}}$ by the factor $[(1-\gamma)J]^n$ and by the number of times the cluster appears in the crystal.

Let us draw a dotted line between two subclusters which interact with each other by having contraction lines that are overlapping or that appear in nearest-neighbor atoms during an overlapping time interval. If any two subclusters of a diagram are connected with each other through dotted lines, the diagram is said to be connected. If not, the diagram is disconnected and should be discarded. Even if a disconnected diagram is included, however, the cumulant average given by Eq. (2.5) becomes zero, thus eliminating possible mistakes in generating diagrams. This is a definite advantage in this formulation.

III. REARRANGEMENT OF CUMULANT CORRECTIONS

The main difficulty in extending the cumulant expansion to an infinite order is that as the number n of variables increases, the number of cumulant corrections increases as $n!$. To overcome the difficulty, let us rearrange the cumulant sum given by Eq. (2.5) such that the values of higher-order cumulants $\langle A_{m+1}A_m\cdots A_1\rangle_{\text{cum}}$ obtained by adding an extra variable A_{m+1} can be calculated immediately, provided A_{m+1} is connected with A_1 only and does not overlap in time with the other variables $A_m, \ldots, A_2$. In Sec. IV–VI we shall discuss how higher-order variables A_{m+1} should be generated so that the method developed in this section can be applied.

Let us first show that $\langle A_{m+1}A_m\cdots A_1\rangle_{\text{cum}}$ can be expanded as

$$\langle A_{m+1}A_m\cdots A_1\rangle_{\text{cum}} = \sum_{l=1}^{m} \sum_{\substack{\text{all possible}\\ l \text{ partitions}}} \sum_{j=1}^{l} (-1)^{l-1}(l-1)!\langle A_{i_1}\cdots\rangle \langle A_{i_2}\cdots\rangle \cdots \langle A_{m+1}[A_{i_j}\cdots]\rangle_{\text{cum}} \cdots \langle A_{i_l}\cdots\rangle \ , \tag{3.1}$$

where the second summation is to include all possible l partitions $A_{i_1}\cdots$, $A_{i_2}\cdots$, $\ldots$, $A_{i_l}\cdots$ of the m variables $A_m, \ldots, A_1$, while the notation

$$\langle A_{m+1}[A_{i_j}\cdots]\rangle_{\text{cum}} \equiv \langle A_{m+1}A_{i_j}\cdots\rangle - \langle A_{m+1}\rangle \langle A_{i_j}\cdots\rangle \tag{3.2}$$

is introduced to represent the cumulant correction between two objects A_{m+1} and $[A_{i_j}\cdots]$.

For instance, the addition of an extra variable, A_3, to the cumulant average

$$\langle A_2A_1\rangle_{\text{cum}} = \langle A_2A_1\rangle - \langle A_2\rangle \langle A_1\rangle \tag{3.3}$$

leads to

$$\langle A_3A_2A_1\rangle_{\text{cum}} = \langle A_3[A_2A_1]\rangle_{\text{cum}} - \langle A_3A_1\rangle_{\text{cum}}\langle A_2\rangle - \langle A_3A_2\rangle_{\text{cum}}\langle A_1\rangle \ , \tag{3.4}$$

as can be proved directly. The more general expression, Eq. (3.1), can be proved as follows. Use of Eq. (3.2) in the expression on the right-hand side of Eq. (3.1) yields

$$\sum_{l=1}^{m} \sum_{l \text{ partitions}} \sum_{j=1}^{l} (-1)^{l-1}(l-1)! \times\langle A_{i_1}\cdots\rangle\cdots\langle A_{m+1}A_{i_j}\cdots\rangle\cdots\langle A_{i_l}\cdots\rangle - \sum_{l=1}^{m} \sum_{l \text{ partitions}} \sum_{j=1}^{l} (-1)^{l-1}(l-1)! \times\langle A_{i_1}\cdots\rangle\cdots\langle A_{i_j}\cdots\rangle\cdots\langle A_{i_l}\cdots\rangle\langle A_{m+1}\rangle \ . \tag{3.5}$$

Since the second term of the above expression is independent of j, the summation $\sum_{j=1}^{l}$ may be replaced by l. Hence this term may be considered as the sum of all possible partitions of $m+1$ variables $A_{m+1}, \ldots, A_1$, in which A_{m+1} always appears alone. The simplest partition is $\langle A_m\cdots A_1\rangle\langle A_{m+1}\rangle$ and hence $l' \equiv l+1$ runs from $l'=2$ to $l'=m+1$. On the other hand, the first term may be regarded as the sum of all possible partitions of the same $m+1$ variables, in which A_{m+1} appears with other A's. The highest partition is of the form $\langle A_m\rangle\langle A_{m-1}\rangle\cdots\langle A_{m+1}A_j\rangle\cdots\langle A_1\rangle$ and hence l runs from $l=1$ to $l=m$. The two terms may then be combined as

$$\sum_{l=1}^{m+1} \sum_{l \text{ partitions}} (-1)^{l-1}(l-1)! \times\langle A_{i_1}\cdots\rangle\langle A_{i_2}\cdots\rangle\cdots\langle A_{i_l}\cdots\rangle \ , \tag{3.6}$$

where $A_{i_1}\cdots$, $A_{i_2}\cdots$, $\ldots$, $A_{i_l}\cdots$ are an l partition of the $m+1$ variables $A_{m+1}, \ldots, A_1$. This expression is exactly the same as the expression on the right-hand side of Eq. (2.5) except that m is replaced by $m+1$. This proves Eq. (3.1).

If the subcluster A_{m+1} is connected with A_1 but does not overlap in time with all the other A's, $\langle A_{m+1}[A_{i_j}\cdots]\rangle_{\text{cum}}$ will vanish unless $A_{i_j}\cdots$ involves A_1. Then Eq. (3.1) is reduced to

$$\langle A_{m+1}A_m\cdots A_1\rangle_{\text{cum}} = \sum_{l=1}^{m} \sum_{\substack{\text{all possible} \\ l \text{ partitions}}} (-1)^{l-1}(l-1)! \times\langle A_{m+1}[A_1A_{i_1}\cdots]\rangle_{\text{cum}} \times\langle A_{i_2}\cdots\rangle\cdots\langle A_{i_l}\cdots\rangle \ , \tag{3.7}$$

where $A_{i_1}\cdots, A_{i_2}\cdots, \ldots, A_{i_l}\cdots$ are an l partition of $m-1$ variables $A_2, \ldots, A_m$. This proves that the contribution Δ_{m+1} of A_{m+1} in $\langle A_{m+1}A_m\cdots A_1\rangle_{\text{cum}}$ is just the cumulant correction between two subclusters A_{m+1} and A_1,

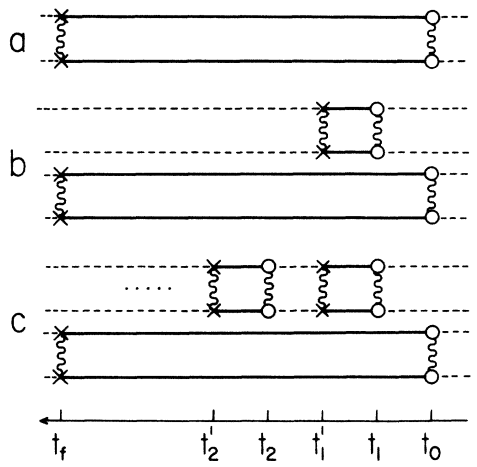

FIG. 1. Simplest examples of self-energy corrections: (a) is the basic diagram; (b) is the simplest self-energy correction to the basic diagram; and (c) illustrates the direct way to add an arbitrary number of times the same correction to the basic diagram.

$$\Delta(A_{m+1}) = \langle A_{m+1}A_1\rangle_{\text{cum}}/\langle A_1\rangle \ . \tag{3.8}$$

The present simplification allows us to extend a summation of certain types of diagrams up to an infinite order, as will be discussed in Secs. IV and V.

IV. INFINITE SUMMATION AND SELF-ENERGY CORRECTIONS

Let us first illustrate, by a simple example, how an infinite series of diagrams can be summed up. The simplest diagram shown in Fig. 1(a) has the value

$$E_0 = -2K_0(1-\gamma)^2(\epsilon-2)^{-1} \ , \tag{4.1a}$$

where

$$K_0 \equiv 2j^2zJN, \quad \epsilon \equiv 4zj \ , \tag{4.1b}$$

and N is the number of atoms on each sublattice, while the diagram composed of two subclusters $A^{(0)}$ and $A_1^{(1)}$ shown in Fig. 1(b) yields the value

$$\Delta E^{(1)}E_0 \ , \tag{4.2a}$$

$$\Delta E^{(1)} \equiv 4j^2(1-\gamma)^2(\epsilon-2)^{-1} \times[(2\epsilon-6)^{-1} - (2\epsilon-4)^{-1}] \ , \tag{4.2b}$$

where the contribution $\Delta E^{(1)}$ of the additional subcluster $A_1^{(1)}$ contains the cumulant correction of the diagram properly. Note that the terms in the square brackets in Eq. (4.2b) is the contribution during the time interval $t_{1'} - t_1$ and the factor $(\epsilon-2)^{-1}$ appears during the interval $t_f - t_{1'}$.

Let us now generate a series of diagrams by adding, one by one, subclusters $A_1^{(1)}$, $A_2^{(1)}$, $\ldots$ which are not overlapping with each other in time as shown in Fig. 1(c). According to Eq. (3.8), the

value of a diagram with $m+1$ additional subclusters, $\langle A_{m+1}^{(I)} A_m^{(I)} \cdots A_1^{(I)} A^{(0)} \rangle_{cum}$, is obtained:

$$\langle A_{m+1}^{(I)} A_m^{(I)} \cdots A_1^{(I)} A^{(0)} \rangle_{cum} = \Delta E^{(I)} \langle A_m^{(I)} \cdots A_1^{(I)} A^{(0)} \rangle_{cum} , \tag{4.3}$$

and hence the sum of the series is calculated as

$$\sum_{m=0}^{\infty} \langle A_m^{(I)} \cdots A_1^{(I)} A^{(0)} \rangle = E_0 \sum_{m=0}^{\infty} [\Delta E^{(I)}]^m$$

$$= E_0 (1 - \Delta E^{(I)})^{-1} . \tag{4.4}$$

It is not necessary to add subclusters to the same pair of atoms. Even if subclusters are added to different but equivalent pairs of atoms around the main diagram $A^{(0)}$, as shown in Fig. 2(a), the value of the diagram remains the same. If there are $p^{(I)}$ equivalent pairs of atoms, the sum of all possible diagrams will be

$$E_0 (1 - p^{(I)} \Delta E^{(I)})^{-1} = -2K_0 (1-\gamma)^2 (\epsilon - 2 - p^{(I)} M^{(I)})^{-1} , \tag{4.5a}$$

where

$$M^{(I)} = (\epsilon - 2) \Delta E^{(I)} . \tag{4.5b}$$

Here we have rewritten the energy expression such that the total contribution of subclusters, $M^{(I)}$, appears in the form of a self-energy correction to the original diagram $A^{(0)}$.

Let us further investigate diagrams of the type shown in Fig. 2(b). The values of such diagrams may be evaluated similarly by dividing them into time intervals where two lines and four lines appear alternatively. The contribution from each time interval is then found to be exactly the same as the contribution from the corresponding time interval in the diagram in Fig. 2(a). Hence the value of the new diagram is the same as that of the diagram in Fig. 2(a) and the sum of the new series of diagrams may also be given by Eq. (4.5). As is illustrated in Fig. 2(c), these two types of subclusters may appear mixed in arbitrary order. Therefore, the total sum of diagrams thus far discussed should be

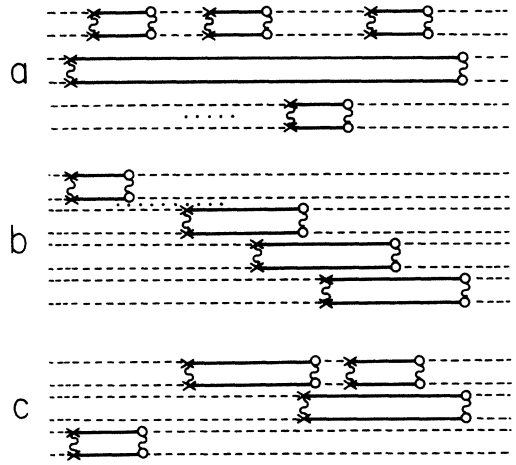

FIG. 2. Examples of self-energy corrections which give the same contribution to the basic diagram: (a) demonstrates that there are many equivalent locations in the basic diagram to which the simplest correction can be added; (b) shows a correction which looks different but yields the same contribution as the simplest correction; (c) illustrates how the two types of corrections can appear mixed in the basic diagram.

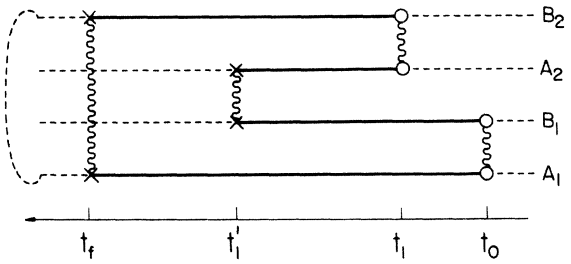

FIG. 3. Example of self-energy corrections which are not separable from the basic diagram. The two horizontal lines linked by a dashed line represent nearest-neighbor atoms in the lattice.

$$E_0 (1 - 2p^{(I)} \Delta E^{(I)})^{-1} = -2K_0 (1-\gamma)^2 (\epsilon - 2 - 2p^{(I)} M^{(I)})^{-1} , \tag{4.6}$$

confirming that $M^{(I)}$ plays the role of self-energy corrections.

Our infinite-order perturbation is a natural extension of the foregoing calculation. We may add to the main diagram $A^{(0)}$ all possible and distinct subclusters $A_\alpha^{(I)}, A_\beta^{(I)}, \ldots$, each of them repeating an arbitrary number of times. If the subclusters are not overlapping with each other in time and interact with $A^{(0)}$ only, the value of such a diagram may again be calculated, step by step, by a relation similar to Eq. (4.3), and the total sum will be written as

$$E = -K_0 + E_0 (1 - E^{(I)})^{-1}$$

$$= -K_0 - 2K_0 (1-\gamma)^2 (\epsilon - 2 - \mathfrak{M}^{(I)})^{-1} , \tag{4.7}$$

where

$$E^{(I)} = p_\alpha^{(I)} \Delta E_\alpha^{(I)} + p_\beta^{(I)} \Delta E_\beta^{(I)} + \cdots , \tag{4.8a}$$

$$\mathfrak{M}^{(I)} = (\epsilon - 2) E^{(I)}$$

$$= p_\alpha^{(I)} M_\alpha^{(I)} + p_\beta^{(I)} M_\beta^{(I)} + \cdots , \tag{4.8b}$$

$$\Delta E_\alpha^{(I)} = \frac{\langle A_\alpha^{(I)} A^{(0)} \rangle_{cum}}{\langle A^{(0)} \rangle} , \tag{4.8c}$$

$$M_\alpha^{(I)} = (\epsilon - 2) \Delta E_\alpha^{(I)} . \tag{4.8d}$$

Here $M_\alpha^{(I)}$ is the portion of self-energy $\mathfrak{M}^{(I)}$ which is created by subclusters of the type $A_\alpha^{(I)}$, and $p_\alpha^{(I)}$ is the number of times that subclusters of the type $A_\alpha^{(I)}$ appear around the main diagram $A^{(0)}$.

"Subclusters" like the one in Fig. 3 may also be added in the summation. Since such a subcluster is connected to the main diagram $A^{(0)}$ through pair-creation or -destruction lines and is inseparable from $A^{(0)}$, it is convenient to define a self-energy correction more generally as follows. Let a self-energy correction be a portion of a diagram between two successive time intervals containing only two spin-deviation lines. The value of a self-energy correction depends on whether or not the incoming two spin-deviation lines occupy nearest-neighbor atoms and also whether or not the outgoing two spin-deviation lines occupy nearest-neighbor atoms. If the two outgoing spin-deviation lines do not occupy nearest-neighbor atoms, their contribution to the self-energy correction is no longer $(\epsilon-2)^{-1}$ but becomes ϵ^{-1}. Hence the energy of the diagrams cannot be summed up in the form of Eqs. (4.7) and (4.8), and, in particular, Eq. (4.8d) should be replaced by

$$M_{\alpha\beta}^{(I)} = (\epsilon - \Delta_\alpha)\Delta E_{\alpha\beta}^{(I)} \quad , \tag{4.9}$$

where $\Delta_\alpha = 2$ if the outgoing lines occupy nearest-neighbor atoms and $\Delta_\alpha = 0$ otherwise. The indices α and β, respectively, identify the type of the self-energy correction as well as the geometrical configurations of the incoming and outgoing lines. $M_\alpha^{(I)}$ introduced in Eq. (4.8) may be written as $M_{\alpha\alpha}^{(I)}$, emphasizing the fact that the incoming and outgoing terminals are the same type.

Self-energy corrections with matching terminals can be added in series as shown in Fig. 4. Let ${}^nQ_{\alpha\beta}^{(I)}$ be the sum of all possible n corrections which have the common incoming and outgoing terminals α and β. Then ${}^{n+1}Q_{\alpha\beta}^{(I)}$ may be computed by the recurrence relation

$${}^{n+1}Q_{\alpha\beta}^{(I)} = \sum_\gamma (\epsilon - \Delta_\alpha)^{-1}\mathfrak{M}_{\alpha\gamma}^{(I)}\,{}^nQ_{\gamma\beta}^{(I)} \quad , \quad {}^0Q^{(I)} = 1 \, , \tag{4.10}$$

which is a generalization of Eq. (4.3). Here $\mathfrak{M}_{\alpha\gamma}^{(I)}$ is the sum of all possible self-energy corrections

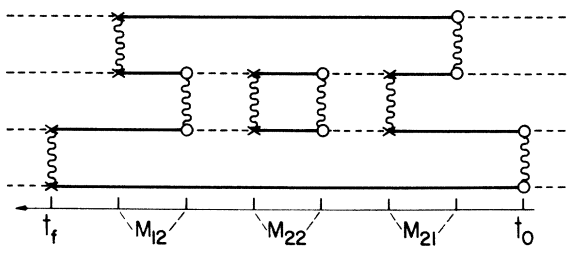

FIG. 4. Self-energy diagrams which have terminals different from those of the simplest corrections.

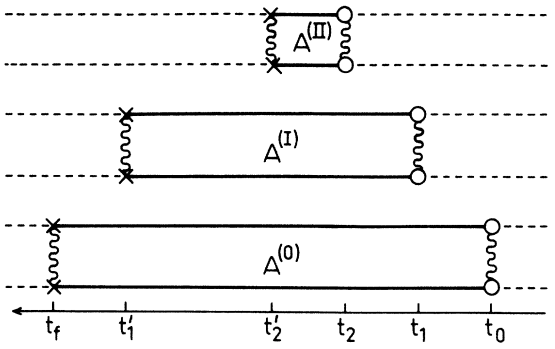

FIG. 5. Example of second-order self-energy corrections.

having fixed terminals α and γ, that is, $\sum p_{\alpha\gamma}^{(I)} M_{\alpha\gamma}^{(I)}$. Summing both sides of Eq. (4.10) in all orders n, we find that

$$\mathfrak{Q}_{\alpha\beta}^{(I)} - \sum_\gamma (\epsilon - \Delta_\alpha)^{-1}\mathfrak{M}_{\alpha\gamma}^{(I)}\mathfrak{Q}_{\gamma\beta}^{(I)} = \delta_{\alpha\beta} \quad , \tag{4.11}$$

where

$$\mathfrak{Q}_{\alpha\beta}^{(I)} \equiv \sum_{n=0}^{\infty} {}^nQ_{\alpha\beta}^{(I)} \tag{4.12}$$

is the sum of corrections in all orders.

Let us regard $\mathfrak{Q}_{\alpha\beta}^{(I)}$ and $\mathfrak{M}_{\alpha\beta}^{(I)}$ as the $\alpha\beta$ elements of matrices $\underline{\mathfrak{Q}}^{(I)}$ and $\underline{\mathfrak{M}}^{(I)}$ and $(\epsilon - \Delta_\alpha)$ as the $\alpha\alpha$ element of the diagonal matrix $(\underline{\epsilon} - \underline{\Delta}^{(I)})$. Then

$$\underline{\mathfrak{Q}}^{(I)} = [1 - (\underline{\epsilon} - \underline{\Delta}^{(I)})^{-1}\underline{\mathfrak{M}}^{(I)}]^{-1} \quad . \tag{4.13}$$

After solving the above equation for $\mathfrak{Q}$, the ground-state energy can be calculated by

$$E = -K_0 + \mathfrak{Q}_{11}^{(I)} E_0 \, . \tag{4.14}$$

As an example, let us consider diagrams of the type shown in Fig. 4. Depending upon the configurations of the incoming and outgoing terminals, there appear four distinct self-energy corrections $M_{11}^{(I)}$, $M_{12}^{(I)}$, $M_{21}^{(I)}$, and $M_{22}^{(I)}$, and hence

$$\underline{\mathfrak{M}}^{(I)} = \begin{pmatrix} p_{11}M_{11}^{(I)} & p_{12}M_{12}^{(I)} \\ p_{21}M_{21}^{(I)} & p_{22}M_{22}^{(I)} \end{pmatrix} \tag{4.15a}$$

and

$$\underline{\epsilon} - \underline{\Delta} = \begin{pmatrix} \epsilon - 2 & 0 \\ 0 & \epsilon \end{pmatrix} \, . \tag{4.15b}$$

The ground-state energy is then calculated as

$$E = -K_0 - 2K_0(1-\gamma)^2(\epsilon - 2 - \mathfrak{M}_{11}^{(I)})^{-1} \quad , \tag{4.16a}$$

$$\mathfrak{M}_{11}^{(I)} = p_{11}^{(I)}M_{11}^{(I)} + p_{12}^{(I)}M_{12}^{(I)} \times (\epsilon - p_{22}^{(I)}M_{22}^{(I)})^{-1}p_{21}^{(I)}M_{21}^{(I)} \quad . \tag{4.16b}$$

V. HIGHER-ORDER SELF-ENERGY CORRECTIONS

Let us further generalize the concept of self-energy corrections introduced in Sec. IV. It is obvious that a self-energy correction may contain repeated portions and hence it would be useful if they can be summed similarly.

We shall again illustrate the method by the simple example shown in Fig. 5. The main diagram consists of two subclusters $A^{(\mathrm{I})}$ and $A^{(0)}$. The third subcluster $A^{(\mathrm{II})}$ does not interact with $A^{(0)}$ directly and $\langle A^{(\mathrm{II})}A^{(0)}\rangle = 0$. Hence the contribution of $A^{(\mathrm{II})}$ may be computed by Eq. (3.7). The result is

$$\langle A^{(\mathrm{II})}A^{(\mathrm{I})}A^{(0)}\rangle_{\mathrm{cum}} = \langle A^{(\mathrm{II})}[A^{(\mathrm{I})}A^{(0)}]\rangle_{\mathrm{cum}} - \langle A^{(0)}\rangle\ \langle A^{(\mathrm{II})}A^{(\mathrm{I})}\rangle_{\mathrm{cum}} \ , \tag{5.1}$$

where

$$\langle A^{(\mathrm{II})}[A^{(\mathrm{I})}A^{(0)}]\rangle_{\mathrm{cum}} = 4j^2(1-\gamma)^2(\epsilon-2)^{-1} \times \Delta E_1^{(\mathrm{II})}(2\epsilon-6)^{-1}E_0 \ , \tag{5.2a}$$

$$\langle A^{(0)}\rangle\ \langle A^{(\mathrm{II})}A^{(\mathrm{I})}\rangle_{\mathrm{cum}} = 4j^2(1-\gamma)^2(\epsilon-2)^{-1} \times \Delta E_2^{(\mathrm{II})}(2\epsilon-4)^{-1}E_0 \ , \tag{5.2b}$$

$$\Delta E_1^{(\mathrm{II})} = 4j^2(1-\gamma)^2(2\epsilon-6)^{-1} \times [(3\epsilon-10)^{-1} - (3\epsilon-8)^{-1}] \ , \tag{5.3a}$$

$$\Delta E_2^{(\mathrm{II})} = 4j^2(1-\gamma)^2(2\epsilon-4)^{-1} \times [(3\epsilon-8)^{-1} - (3\epsilon-6)^{-1}] \ . \tag{5.3b}$$

In this example, the self-energy correction defined in Sec. IV appears during the time interval $t_f - t_1$ and is given by the difference between the two quantities in Eq. (5.2) divided by E_0. On the other hand, the contribution of $A^{(\mathrm{II})}$, which appears during the time interval $t_1 - t_2$, varies depending upon whether or not $A^{(\mathrm{I})}$ and $A^{(0)}$ are connected; the value will be $\Delta E_1^{(\mathrm{II})}$ when $A^{(\mathrm{I})}$and $A^{(0)}$ are connected as in Eq. (5.2a), but $\Delta E_2^{(\mathrm{II})}$ when $A^{(\mathrm{I})}$ and $A^{(0)}$ are disconnected as in Eq. (5.2b). This would introduce a new complication in extending the calculation to an infinite order, but we can handle it as follows.

Let $A_m^{(\mathrm{II})}$ be the mth correction added to the main diagram $A^{(\mathrm{I})}A^{(0)}$. If m corrections $A_m^{(\mathrm{II})}A_{m-1}^{(\mathrm{II})} \cdots A_1^{(\mathrm{II})}$ are not overlapping with each other in time and do not interact with $A^{(0)}$ directly, the cumulant average may be divided into parts by Eq. (3.7) as follows:

$$\langle A_m^{(\mathrm{II})}\cdots A_1^{(\mathrm{II})}A^{(\mathrm{I})}A^{(0)}\rangle_{\mathrm{cum}} = \langle A_m^{(\mathrm{II})}\cdots A_1^{(\mathrm{II})}[A^{(\mathrm{I})}A^{(0)}]\rangle_{\mathrm{cum}} - \langle A^{(0)}\rangle\ \langle A_m^{(\mathrm{II})}\cdots A_1^{(\mathrm{II})}A^{(\mathrm{I})}\rangle_{\mathrm{cum}} \ . \tag{5.4}$$

The two cumulants on the right-hand side of Eq. (5.4) can be computed separately by Eq. (4.7) and the sum of the series may be written as

$$\sum_{m=0}^{\infty}\langle A_m^{(\mathrm{II})}\cdots A_1^{(\mathrm{II})}A^{(\mathrm{I})}A^{(0)}\rangle_{\mathrm{cum}} = (1-\Delta E_1^{(\mathrm{II})})^{-1}\langle A^{(\mathrm{I})}A^{(0)}\rangle - (1-\Delta E_2^{(\mathrm{II})})^{-1}\langle A^{(\mathrm{I})}\rangle\ \langle A^{(0)}\rangle = 4j^2(1-\gamma)^2[(2\epsilon-6-M_1^{(\mathrm{II})})^{-1} - (2\epsilon-4-M_2^{(\mathrm{II})})^{-1}]E_0 \ , \tag{5.5}$$

where

$$M_1^{(\mathrm{II})} = p^{(\mathrm{II})}(2\epsilon-6)\Delta E_1^{(\mathrm{II})} \tag{5.6a}$$

and

$$M_2^{(\mathrm{II})} = p^{(\mathrm{II})}(2\epsilon-8)\Delta E_2^{(\mathrm{II})} \tag{5.6b}$$

are the self-energy corrections for $\langle A^{(\mathrm{I})}A^{(0)}\rangle$ and $\langle A^{(\mathrm{I})}\rangle\ \langle A^{(0)}\rangle$, respectively. We can of course calculate the sum of diagrams generated by adding many subclusters $A^{(\mathrm{I})}$, each of which contains $A_m^{(\mathrm{II})}\cdots A_1^{(\mathrm{II})}$. The calculation can also be extended by adding higher-order corrections $A_1^{(\mathrm{III})}A_2^{(\mathrm{III})}\cdots$ to each of the subclusters of type $A^{(\mathrm{II})}$, etc. If we continue to extend the calculation in this manner but if we exclude diagrams which have distinct incoming and outgoing terminals, $M_{\alpha\beta}$ $(\alpha\neq\beta)$, the total sum will be written in the form[13]

$$E = -K_0 - 2K_0(1-\gamma)^2/\delta E$$

$$\delta E \equiv \epsilon - 2 - f_1 \Big/ \left(2\epsilon - 6 - \frac{f_2}{3\epsilon - 10 - (f_3/4\epsilon - \cdots) - (f_3/4\epsilon - \cdots)} - \frac{f_2}{3\epsilon - 8 - (f_3/4\epsilon - \cdots) - (f_3/4\epsilon - \cdots)}\right)$$

$$- f_1 \Big/ \left(2\epsilon - 4 - \frac{f_2}{3\epsilon - 8 - (f_3/4\epsilon - \cdots) - \cdots} - \frac{f_2}{3\epsilon - 6 - (f_3/4\epsilon - \cdots) - \cdots}\right) \ , \tag{5.7}$$

where $f_J = 4j^2(1-\gamma)^2 p^{(J)}$ and $p^{(J)}$ is the number of times that subclusters of the type $A^{(J)}$ appear around the diagram $A^{(J-1)}$.

The foregoing calculation suggests that subclusters $A^{(II)}\cdots$ are self-energy corrections to the original self-energy $M^{(I)}$. We may call this type of correction second-order self-energy corrections and denote them by $\mathfrak{M}^{(II)} = \sum p^{(II)} M^{(II)}$. We can further introduce higher-order corrections $\mathfrak{M}^{(III)}$, $\mathfrak{M}^{(IV)}$, etc.

By definition, the simplest possible time interval in any first-order self-energy correction $M^{(I)}$ contains at least four spin-deviation lines. A second-order self-energy correction is then defined more generally as a portion of a diagram between two successive time intervals which contain only four spin deviations. Hence a second-order self-energy correction itself consists of at least six spin-deviation lines and its value depends on how these lines are connected. Let us denote the value of a second-order self-energy diagram

$$M^{(II)}_{\alpha h,\beta l} = M^{(II)(c)}_{\alpha h,\beta l} - M^{(II)(nc)}_{\alpha h,\beta l} \quad , \tag{5.8}$$

where the index h (or l) denotes whether the four outgoing lines at the terminal α (or the four incoming lines at β) belong to two separate subclusters or not and, if so, h (or l) also denotes whether the subclusters are connected or not. This information is automatically transferred from diagram to diagram through the matrix multiplication. In addition, $M^{(c)}$ and $M^{(nc)}$ illustrate whether the subcluster A_α involving the two spin-deviation lines that are terminated at the terminal α is connected with the four incoming lines of the diagram or not. If A_α is a simple subcluster like the example in Fig. 5, the cumulant correction associated with A_α may be calculated by Eq. (5.8).

Self-energy diagrams with matching terminals can now be added in series. The sum of all possible second-order self-energy corrections $Q^{(II)}_{\alpha h,\beta l}$, which have the common incoming and outgoing terminals αh and βl, is then obtained by

$$\mathfrak{Q}^{(II)}_{\alpha h,\beta l} - \sum_{\gamma k} (2\epsilon - \Delta_{\alpha h})^{-1} \mathfrak{M}^{(II)}_{\alpha h,\gamma k} \mathfrak{Q}^{(II)}_{\gamma k,\beta l} = \delta_{\alpha h,\beta l} \tag{5.9}$$

or

$$\underline{\mathfrak{Q}}^{(II)} = [1 - (2\underline{\epsilon} - \underline{\Delta}^{(II)})^{-1} \underline{\mathfrak{M}}^{(II)}]^{-1} \quad , \tag{5.10}$$

where $\mathfrak{M}^{(II)}_{\alpha h,\gamma k}$ is the sum of all possible second-order self-energy corrections $M^{(II)}_{\alpha h,\gamma k}$. The above equations correspond to Eq. (4.11) and (4.13) and $\mathfrak{Q}^{(II)}$, $\mathfrak{M}^{(II)}$, and $(2\underline{\epsilon} - \underline{\Delta}^{(II)})$ are matrices whose $\alpha h, \beta l$ elements are given by $\mathfrak{Q}^{(II)}_{\alpha h,\beta l}$, $\mathfrak{M}^{(II)}_{\alpha h,\beta l}$, and $(2\epsilon - \Delta_{\alpha h})\,\delta_{\alpha h,\beta l}$, respectively.

We note that the cumulant correction contained in the subcluster A_α terminated at time $t_{2'}$ is not necessarily given by Eq. (5.8). This happens when A_α extends beyond the self-energy diagram as in the example in Fig. 6. In such a case, whether A_α is connected to the rest of the diagram or not may be determined automatically by the fact that the two incoming subclusters are connected with each other or not. Let us denote by $\gamma k'$ and $\gamma k''$ two corresponding situations; that is, the two incoming subclusters are connected in $\gamma k'$ but disconnected in $\gamma k''$. Then $M^{(II)(c)}_{\alpha h,\gamma k'} = M^{(II)(nc)}_{\alpha h,\gamma k'} = 0$ and the cumulant correction relevant to A_α is given by

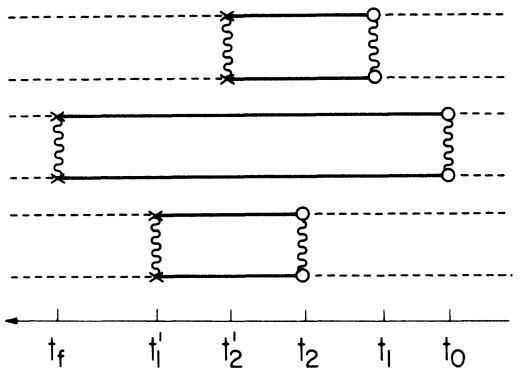

FIG. 6. Cumulant corrections involved in complex self-energy corrections.

$$M^{(II)}_{\alpha h,\gamma k'} \mathfrak{Q}^{(II)}_{\gamma k',\beta l} + M^{(II)}_{\alpha h,\gamma k''} \mathfrak{Q}^{(II)}_{\gamma k'',\beta l}$$

$$= M^{(II)(c)}_{\alpha h,\gamma k'} \mathfrak{Q}^{(II)}_{\gamma k',\beta l} - M^{(II)(nc)}_{\alpha h,\gamma k''} \mathfrak{Q}^{(II)}_{\gamma k'',\beta l} \quad . \tag{5.11}$$

Since Eqs. (5.9) and (5.10) already contain this difference, solutions $\mathfrak{Q}^{(II)}$ always include cumulant corrections for terminating subclusters A_α properly.

In the example in Fig. 5, the incoming and outgoing subclusters are both connected or both disconnected and there are no cross terms. Hence the matrix equation (5.10) is diagonal, yielding the result, Eq. (5.5), consisting of two terms.

The cumulant correction between two outgoing subclusters may be included properly when the first-order self-energy correction is calculated by

$$M^{(I)}_{\alpha\beta} = 4(j - n_{\alpha'})\,(j - n_{\alpha''})\,(1-\gamma^2)\,(Q^{(II)}_{\alpha h',\beta l} - Q^{(II)}_{\alpha h'',\beta l})\,(2\epsilon - \Delta_{\beta l})^{-1} \quad , \tag{5.12}$$

where the two outgoing subclusters are connected in $Q^{(II)}_{\alpha h',\beta l}$ but disconnected in $Q^{(II)}_{\alpha h'',\beta l}$. In case the four outgoing lines belong to a single subcluster, $Q^{(II)}_{\alpha h'',\beta l} = 0$.

If there are more than one contraction lines overlapping in time at the same atomic site, we need to determine the values of $n_{\alpha'}$ and $n_{\alpha''}$ in Eq. (5.12) according to the instruction (ivb) in Sec. II. The same factor n will also appear in $M^{(II)}$. Since a contraction line may extend many self-energy diagrams, this would introduce some additional dif-

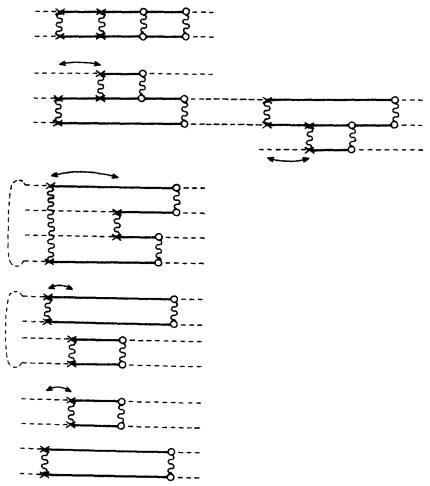

FIG. 7. All possible diagrams in the fourth-order perturbation. The double-headed arrows indicate that the diagrams obtained by interchanging the times of the indicated pairs should also be included.

ficulties in solving Eq. (5.10). However, this equation is quite general and it can be extended in calculating higher-order self-energy corrections $M^{(III)}$, $M^{(IV)}$, ... without introducing any new concept.

VI. NUMERICAL RESULTS AND DISCUSSIONS

We shall now demonstrate how the foregoing method can be applied in calculating an infinite series of diagrams that are involved in the antiferromagnetic ground-state energy.

To avoid possible omission of important lower-order diagrams, let us first examine the results of a finite perturbation expansion. Previously,[11] we have generated by computer all possible diagrams in the second-, fourth-, and sixth-order perturbations and tabulated the ground-state energy in the form

$$E = -K_0[1 + C_1(1-\gamma)^2 + C_2(1-\gamma)^4 + C_3(1-\gamma)^6 + \cdots] , \tag{6.1}$$

where $K_0 \equiv 2j^2 z\, JN$ and C_1, C_2, and C_3 are the sums in unit K_0 of all diagrams in the second, fourth, and sixth perturbations.

The second-order diagram is the trivial one shown in Fig. 1(a). The fourth-order terms consist of five diagrams shown in Fig. 7, and the portion between the time interval $t_{1'} - t_1$ of each fourth-order diagram yields a self-energy correction $M_{11}^{(I,4)}$ which has two incoming lines and two outgoing lines, occupying neighboring atoms. By using relations like Eq. (4.2), the sum of the fourth-order diagrams $\delta E_0^{(4)}$ may be written as

$$\delta E_0^{(4)} = (\epsilon - 2)^{-1} \mathfrak{M}_{11}^{(I,4)} E_0, \qquad \mathfrak{M}_{11}^{(I,4)} = \sum p^{(I)} M_{11}^{(I,4)} . \tag{6.2}$$

According to Eq. (6.1), this value should be equal to $-K_0C_2(1-\gamma)^4$, while $E_0 = -K_0C_1(1-\gamma)^2$. Hence the sum of the self-energy diagrams, $\mathfrak{M}_{11}^{(I,4)}$, is given in terms of C_1 and C_2 as follows:

$$\mathfrak{M}_{11}^{(I,4)} = (\epsilon - 2)\,(1-\gamma)^2 C_2/C_1 . \tag{6.3}$$

Since the matrix $\mathfrak{L}^{(I,4)}$ is one dimensional in the present approximation, the ground-state energy is calculated by Eqs. (4.13) and (4.14) as

$$E_\infty^{(4)} = -K_0 + [1 - (\epsilon - 2)^{-1} \mathfrak{M}_{11}^{(I,4)}]^{-1} E_0 = -K_0 - \frac{-K_0 C_1 (1-\gamma)^2}{1 - (C_2/C_1)\,(1-\gamma)^2} . \tag{6.4}$$

This result corresponds to the sum of all possible diagrams which can be generated by adding, an arbitrary number of times, self-energy diagrams of the types shown in Fig. 7.

Sixth-order diagrams consist of three pair-creation and three pair-destruction operators and may be classified into three types of diagrams illustrated in Fig. 8. Here self-energy corrections $M_{12}^{(I,6)}$, $M_{21}^{(I,6)}$, and $M_{11}^{(I,4)}$ in the second and third diagrams consist of four spin-deviation lines and are irreducible. Self-energy corrections $M_{11}^{(I,6)}$ in the first diagram contain time intervals with six spin-deviation lines, which can be considered as second-order self-energy corrections $M^{(II)}$, but, for simplicity, we shall not sum over these second-order corrections in the following.

The second and third diagrams in Fig. 8 are reducible and, in particular, since the third diagrams have been included in the fourth-order result, Eq. (6.4), we have to omit them. For this purpose, let us first decompose the sum of all diagrams in sixth order, $\delta E_0^{(6)}$, as follows:

$$\delta E_0^{(6)} = (\epsilon - 2)^{-1} \mathfrak{M}_{11}^{(I,6)} E_0 + (\epsilon - 2)^{-1} \mathfrak{M}_{12}^{(I,6)} \epsilon^{-1} \mathfrak{M}_{21}^{(I,6)} E_0 + (\epsilon - 2)^{-1} \mathfrak{M}_{11}^{(I,4)} (\epsilon - 2)^{-1} \mathfrak{M}_{11}^{(I,4)} E_0 . \tag{6.5}$$

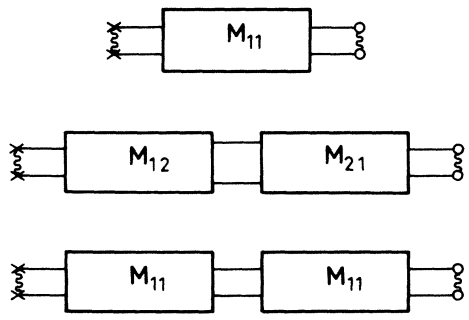

FIG. 8. Three types of second-order self-energy corrections which appear in the sixth-order perturbation.

TABLE I. Ground-state energies of spins coupled by the isotropic exchange interaction γ, in units of $-K_0 = -2j^2zJN$.

Lattice		$j=\frac{1}{2}$ E	$10^3\,\Delta E$ [a]	$j=1$ E	$10^3\,\Delta E$ [a]	$j=\frac{3}{2}$ E	$10^3\,\Delta E$ [a]	$j=2$ E	$10^3\,\Delta E$ [a]	$j=\frac{5}{2}$ E	$10^3\,\Delta E$ [a]
chain	$E_0^{(4)}$	1.7500	−2500	1.3759	426	1.2300	300	1.1658	229	1.1296	185
	$E_\infty^{(4)}$	1.8000	500	1.3821	62	1.2352	52	1.1701	43	1.1332	36
	$E_0^{(6)}$	1.7500	0	1.3837	78	1.2403	103	1.1743	85	1.1367	71
	$E_\infty^{(6)}$	1.7619	119	1.3852	15	1.2436	33	1.1773	30	1.1393	26
plane	$E_0^{(4)}$	1.3314	−19	1.1555	126	1.1008	99	1.0745	78	1.0591	65
	$E_\infty^{(4)}$	1.3314	0	1.1567	12	1.1020	12	1.0755	10	1.0600	9
	$E_0^{(6)}$	1.3345	31	1.1591	36	1.1038	30	1.0770	25	1.0612	21
	$E_\infty^{(6)}$	1.3345	0	1.1597	6	1.1045	7	1.0776	6	1.0617	5
sc	$E_0^{(4)}$	1.1993	−7	1.0964	55	1.0633	45	1.0472	37	1.0376	31
	$E_\infty^{(4)}$	1.1993	0	1.0967	3	1.0636	3	1.0475	3	1.0379	3
	$E_0^{(6)}$	1.2013	20	1.0978	14	1.0645	12	1.0481	9	1.0384	8
	$E_\infty^{(6)}$	1.2013	0	1.0980	2	1.0647	2	1.0482	1	1.0385	1
bcc	$E_0^{(4)}$	1.1478	49	1.0717	50	1.0472	37	1.0352	29	1.0280	24
	$E_\infty^{(4)}$	1.1479	1	1.0721	4	1.0475	3	1.0354	2	1.0282	2
	$E_0^{(6)}$	1.1494	16	1.0730	13	1.0482	10	1.0360	8	1.0286	6
	$E_\infty^{(6)}$	1.1495	1	1.0732	2	1.0484	2	1.0361	1	1.0287	1

[a] ΔE represents energy depreciations, that is, $\Delta E = E_0^{(4)} - E_0^{(2)}$ for $E_0^{(4)}$, $E_\infty^{(4)} - E_0^{(4)}$ for $E_\infty^{(4)}$, $E_0^{(6)} - E_0^{(4)}$ for $E_0^{(6)}$, and $E_\infty^{(6)} - E_0^{(6)}$ for $E_\infty^{(6)}$.

As before, this value should be equal to the last term in Eq. (6.1), that is, $-K_0C_3(1-\gamma)^6$. Since $\mathfrak{M}_{11}^{(I,4)}$ is given by Eq. (6.3), the remainder in Eq. (6.5) is

$$\mathfrak{M}_{11}^{(I,6)} + \mathfrak{M}_{12}^{(I,6)}\epsilon^{-1}\mathfrak{M}_{21}^{(I,6)} = (\epsilon - 2)\,(1-\gamma)^4[(C_3/C_1 - (C_2/C_1)^2] \quad , \tag{6.6}$$

where $\mathfrak{M}_{11}^{(I,6)}$, $\mathfrak{M}_{12}^{(I,6)}$, and $\mathfrak{M}_{21}^{(I,6)}$ are the sums of all possible self-energy corrections found in sixth-order perturbation but it does not include $\mathfrak{M}_{11}^{(I,4)}$ calculated in fourth-order perturbation.

The total contribution to self-energy corrections, $\mathfrak{M}_{11}^{(I)}$, is given by Eq. (4.16b), but up to the sixth-order perturbation, there is no diagram contributing to $M_{22}^{(I)}$. Hence $\mathfrak{M}_{11}^{(I)}$ should be given by the sum of the quantities in Eqs. (6.3) and (6.6), and the ground-state energy may be calculated by

$$E_\infty^{(6)} = -K_0 - \frac{K_0C_1(1-\gamma)^2}{1-(C_2/C_1)\,(1-\gamma)^2 - [(C_3/C_1) - (C_2/C_1)^2]\,(1-\gamma)^4} \quad . \tag{6.7}$$

This result corresponds to the sum of all possible diagrams which can be generated by adding, an arbitrary number of times, self-energy corrections of the types illustrated in Fig. 8.

The long-range order ξ and short-range order η defined by

$$\xi = (2jN)^{-1}\left(\sum_a \langle S_a^z\rangle + \sum_b \langle S_b^z\rangle\right) \quad , \tag{6.8}$$

$$\eta = (2jN)^{-1}\sum_{(ab)} \langle S_a^z S_b^z\rangle \tag{6.9}$$

may be reduced to the following form by using Feynman's theorem[14]:

$$\xi = 1 - \frac{\epsilon}{2K_0}\,\frac{\partial E}{\partial \epsilon} \quad , \tag{6.10}$$

$$\eta = \frac{1}{K_0}\left(E - (1-\gamma)\,\frac{\partial E}{\partial \gamma}\right) \quad . \tag{6.11}$$

The above equations may be calculated easily by inserting the expression for $E_\infty^{(4)}$ or $E_\infty^{(6)}$ in Eq. (6.4) or (6.7). Previously, the differentiations of C_l with respect to ϵ have been performed by computer using the algebraic expressions obtained for the C's, and the values for C and $-(\epsilon/2)\partial C/\partial\epsilon$ are tabulated in Tables II and III of Parrinello, Scire, and Arai[11] (PSA). Use of these values in Eqs. (6.4), (6.7), (6.10), and 6.11) yields the values of $E_\infty^{(4)}$, $E_\infty^{(6)}$, η, and ξ as tabulated in Tables I–III.

The results show an interesting tendency of the Heisenberg magnets. As expected, the one-dimen-

TABLE II. Values of long-range ordering parameter $\xi(E)$.

Lattice		$j=\frac{1}{2}$	$j=1$	$j=\frac{3}{2}$	$j=2$	$j=\frac{5}{2}$
chain	$E_0^{(4)}$	−0.2500	0.6345	0.8113	0.8726	0.9039
	$E_\infty^{(4)}$	−0.1200	0.5942	0.7887	0.8565	0.8913
	$E_0^{(6)}$	−0.3125	0.5481	0.7639	0.8411	0.8802
	$E_\infty^{(6)}$	−0.2335	0.5204	0.7400	0.8235	0.8662
plane	$E_0^{(4)}$	0.7422	0.8914	0.9323	0.9509	0.9615
	$E_\infty^{(4)}$	0.7427	0.8867	0.9284	0.9478	0.9588
	$E_0^{(6)}$	0.7233	0.8778	0.9226	0.9435	0.9555
	$E_\infty^{(6)}$	0.7225	0.8739	0.9192	0.9406	0.9531
sc	$E_0^{(4)}$	0.8720	0.9397	0.9610	0.9712	0.9772
	$E_\infty^{(4)}$	0.8721	0.9385	0.9598	0.9702	0.9764
	$E_0^{(6)}$	0.8646	0.9350	0.9575	0.9685	0.9750
	$E_\infty^{(6)}$	0.8643	0.9341	0.9566	0.9678	0.9744
bcc	$E_0^{(4)}$	0.9055	0.9556	0.9711	0.9787	0.9831
	$E_\infty^{(4)}$	0.9047	0.9544	0.9701	0.9779	0.9824
	$E_0^{(6)}$	0.8995	0.9517	0.9683	0.9765	0.9814
	$E_\infty^{(6)}$	0.8987	0.9508	0.9675	0.9759	0.9809

sional cases are different from others although the differences are rather qualitative. On the other hand, the spin-$\frac{1}{2}$ cases ($j=\frac{1}{2}$) exhibit a distinct tendency and, in particular, the spin-$\frac{1}{2}$ one-dimensional case ($j=\frac{1}{2}$, $z=2$), having the two odd factors mixed in, exhibits a very unique feature.

In case spins are greater than $\frac{1}{2}$, there is the general tendency that as the dimensionality z decreases the contribution from higher-order diagrams increases. More specifically, let us consider how the fourth-order results, $E_0^{(4)}$, $\xi(E_0^{(4)})$, and $\eta(E_0^{(4)})$, based on the five diagrams in Fig. 7 can be improved. One way is to generate all possible diagrams in the sixth order and to find the expression (6.1). As has been discussed in PSA, such a calculation is very involved since numerous diagrams appear and many cancellations take place among them. Another way is to generate an infinite number of diagrams, just repeating the type of diagrams found in the fourth-order calculation. The resulting expression in Eq. (6.4) is trivial to compute. In the two- and three-dimensional cases, the improvements found in the second approach, $E_\infty^{(4)}-E_0^{(4)}$, $\xi(E_\infty^{(4)})-\xi(E_0^{(4)})$, and $\eta(E_\infty^{(4)}-\eta(E_0^{(4)})$, are about $\frac{1}{3}$ of those found in the first approach, $E_0^{(6)}-E_0^{(4)}$, $\xi(E_0^{(6)})-\xi(E_0^{(4)})$, and $\eta(E_0^{(6)})-\eta(E_0^{(4)})$. However, the contributions are both small, suggesting that the fourth-order results $E_0^{(4)}$, $\xi(E_0^{(4)})$, and $\eta(E_0^{(4)})$ are already nearly satisfactory. On the other hand, in the one-dimensional case, the correlation effect becomes appreciable, and, in particular, the ratio between the improvements obtained by the second and first approaches is about 0.8 for $z=1$ and about $\frac{1}{2}$ for $z>\frac{3}{2}$, suggesting that a considerable improvement can be obtained without generating higher-order irreducible diagrams and instead by simply repeating the self-energy diagrams shown in Fig. 7.

The above results will lead to the following conclusion. Among diagrams in the sixth order, those belonging to the last term on the right-hand side of Eq. (6.5) are included in $E_\infty^{(4)}$ exactly, and as the dimensionality decreases the contribution increases and becomes dominant in the one-dimensional case, while the effect of other diagrams, which are newly found in the sixth-order perturbation, remains relatively small. Consequently, it seems more efficient to keep the number of basic diagrams small and to extend the summation to an infinite order, rather than spending a large effort in generating higher order irreducible diagrams.

In spin-$\frac{1}{2}$ cases, spins behave like fermions and try to avoid each other. In two- and three-dimensional cases, this tendency may be taken into account by diagrams which extend to larger space, and in which spin deviations do not appear repeatedly at the same atomic site. An effective interaction between two sites, a and b, is then introduced indirectly through neighboring atoms which connect the two sites a and b. This may be the reason that the contribution from irreducible diagrams in the sixth-order perturbation is dominant while the effects of the infinite summations, $E_\infty^{(4)}-E_0^{(4)}$ and $E_\infty^{(6)}-E_0^{(6)}$, are nearly absent for these cases.

In the spin-$\frac{1}{2}$ one-dimensional case, the indirect interaction cannot appear since there are no neigh-

TABLE III. Values of short-range ordering parameter $\eta(E)$.

Lattice		$j=\frac{1}{2}$	$j=1$	$j=\frac{3}{2}$	$j=2$	$j=\frac{5}{2}$
chain	$E_0^{(4)}$	0.7500	0.5389	0.7100	0.7884	0.8334
	$E_\infty^{(4)}$	0.6000	0.5058	0.6816	0.7648	0.8134
	$E_0^{(6)}$	0.7500	0.4999	0.6585	0.7459	0.7979
	$E_\infty^{(6)}$	0.6734	0.4883	0.6329	0.7224	0.7772
plane	$E_0^{(4)}$	0.6724	0.8193	0.8794	0.9099	0.9279
	$E_\infty^{(4)}$	0.6723	0.8129	0.8730	0.9044	0.9230
	$E_0^{(6)}$	0.6569	0.8013	0.8644	0.8974	0.9174
	$E_\infty^{(6)}$	0.6569	0.7963	0.8592	0.8926	0.9131
sc	$E_0^{(4)}$	0.8021	0.8926	0.9277	0.9454	0.9562
	$E_\infty^{(4)}$	0.8020	0.8907	0.9257	0.9436	0.9546
	$E_0^{(6)}$	0.7921	0.8856	0.9217	0.9409	0.9522
	$E_\infty^{(6)}$	0.7920	0.8863	0.9203	0.9398	0.9511
bcc	$E_0^{(4)}$	0.8424	0.9183	0.9454	0.9590	0.9675
	$E_\infty^{(4)}$	0.8415	0.9162	0.9436	0.9575	0.9659
	$E_0^{(6)}$	0.8344	0.9118	0.9404	0.9550	0.9642
	$E_\infty^{(6)}$	0.8334	0.9103	0.9391	0.9539	0.9634

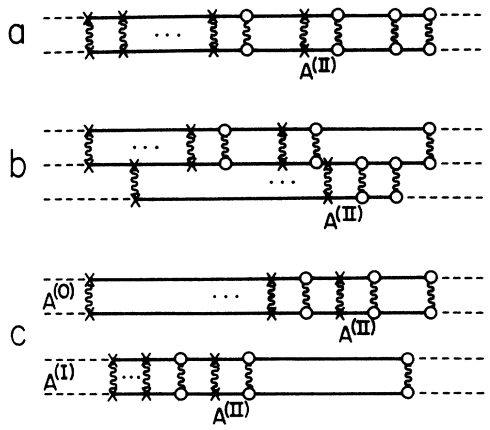

FIG. 9. Second-order self-energy corrections included in the calculation of the linear chain.

boring atoms which connect two sites a and b indirectly and diagrams available for inducing an effective interaction are limited to those with multiple spin deviations at the same site. Since cumulant corrections involved in multiple spin deviations are nonvanishing even for $j=\frac{1}{2}$, these diagrams contribute, but they overestimate spin-flip processes. For instance, the second-order diagram in Fig. 1 leads to $\xi=0$, indicating the disappearance of long-range ordering. The fourth-order diagrams involving double spin deviations at the same site further increase zero-point fluctuations, yielding $\xi=-0.25$. The negative value for ξ is unphysical since it indicates that zero-point fluctuations become greater than the value of spins, $\frac{1}{2}$, effectively reversing all spins in the chain from the unperturbed state $\alpha\beta\alpha\beta\cdots$ to $\beta\alpha\beta\alpha\cdots$. The sixth-order calculation worsens the situation by increasing the negative value of ξ to -0.3125. The reason for this failure is the same; many of the sixth-order diagrams contain double spin deviations at the same site. On the other hand, the infinite summation based on the fourth-order diagrams reduces the negative value of ξ to -0.12. The reason is that the second correction tends to bring the spin ordering back to the original ordering $\alpha\beta\alpha\beta\cdots$, and although the third correction reverse it to $\beta\alpha\beta\alpha\cdots$, the fourth correction again tends to bring it back to $\alpha\beta\alpha\beta\cdots$, and so on. This suggests that the difficulty may be removed by repeating multiple spin deviations further. To calculate correctly the value of ξ, we have to calculate self-energy corrections in the second order, third order, and so on, by Eq. (5.7) as is discussed in Sec. V.

In order to demonstrate the above arguments in practice, we have calculated the contribution of the second-order self-energy corrections shown in Fig. 9. These corrections are assumed to be added to the fourth-order diagrams in Fig. 7 one by one. In the spin-$\frac{1}{2}$ one-dimensional case, Eq. (5.7) is then reduced to

$$E_\infty^{(II)} = -K_0 - \frac{K_0 C_1 (1-\gamma)^2}{1-(C_2^*/C_1)(1-\gamma)^2}\ , \tag{6.12}$$

$$\frac{C_2^*}{C_1} = -\left(\frac{4}{\epsilon-2+\frac{2}{3}(1-\gamma)^2/(\epsilon-2)} + \frac{1}{\epsilon-2+(1-\gamma)^2/(\epsilon-2)} - \frac{2}{\epsilon-3+1/(3\epsilon-8)}\right)\frac{1}{(\epsilon-2)}\ , \tag{6.13}$$

yielding the following values:

$$E_\infty^{(II)} = -1.7954K_0\ , \tag{6.14}$$

$$\xi(E_\infty^{(II)}) = 0.1726\ . \tag{6.15}$$

This example demonstrates how the negative value for ξ can be removed, but the above values should not be taken seriously; it is obvious that the perturbation series for the chain does not converge well and the addition of the third-order self-energy corrections will reduce the value of ξ considerably. A definite conclusion on the value of ξ may be obtained only after a more systematic treatment of higher-order terms based on the present method, which is beyond the scope of this paper. There exists an exact solution for the linear chain,[15] but the long-range ordering ξ cannot be calculated from the exact solution.[16]

In conclusion, when spins are greater than $\frac{1}{2}$, the system behaves like that of bosons and diagrams, which contain simple self-energy corrections repeatedly, contribute to the ground-state properties predominantly, making the present infinite-cumulant-expansion method very valuable. When spins are $\frac{1}{2}$, the system behaves like that of fermions and requires quite different classes of diagrams, suggesting that the spin-spin correlations are distinctively different in these two cases.

*Based on work performed under the auspices of the U. S. Atomic Energy Commission.

[1]G. P. Felcher, T. Arai, G. H. Lander, S. K. Sinha, and F. H. Spedding (unpublished); also see, T. Arai and G. P. Felcher, Bull. Am. Phys. Soc. 18, 398 (1973).

[2]R. E. Walstedt, H. W. de Wijn, and H. J. Guggenheim, Phys. Rev. Lett. 25, 1119 (1970); H. E. de Wijn, R. E. Walstedt, L. R. Walker, and H. J. Guggenheim, J. Appl. Phys. 42, 1595 (1971); H. W. de Wijn, L. R. Walker, and R. E. Walstedt, Phys. Rev. B 8, 285 (1973).

[3]P. W. Anderson, Phys. Rev. 86, 694 (1952); R. Kubo, Phys. Rev. 87, 568 (1952).

[4]L. R. Walker, in *Proceedings of the International Conference on Magnetism, Nottingham*, 1964 (Institute of Physics and the Physical Society, London, 1965), p. 21.

[5]H. L. Davis, Phys. Rev. 120, 789 (1960).

[6]F. J. Dyson, Phys. Rev. 102, 1217 (1956); *ibid.* 102, 1230 (1956).

[7]R. B. Stinchcombe, G. Horwitz, F. Englert, and R. Brout, Phys. Rev. 130, 155 (1963).

[8]M. H. Boon, Nuovo Cimento 21, 885 (1961); Y. L. Wang, S. Shtrikman, and H. Callen, Phys. Rev. 148, 419 (1966); also see Y. L. Wang and H. B. Callen, Phys. Rev. 148, 433 (1966).

[9]T. Arai and B. Goodman, Phys. Rev. 155, 514 (1967).

[10]R. Kubo, J. Phys. Soc. Jap. 17, 1100 (1962).

[11]M. Parrinello, M. Scire, and T. Arai, Nuovo Cimento Lett. 6, 138 (1973); this paper will be referred to as PSA.

[12]For bosons, see J. L. De Coen, F. Englert, and R. Brout, Physica 30, 1293 (1964).

[13]This result corresponds to a generalization of the continued-fraction representation of the time correlation functions by H. Mori, Prog. Theor. Phys. 34, 399 (1965).

[14]R. Feynman, Phys. Rev. 56, 340 (1939).

[15]L. Hulthén, Ark. Mat. Astron. Fys. 26A, 1 (1938); R. Orbach, Phys. Rev. 112, 309 (1958).

[16]See L. R. Walker, Phys. Rev. 116, 1089 (1959). He has expanded the analytical solution of the anisotropic Heisenberg Hamiltonian obtained by Orbach (Ref. 15) and compared it term by term with the perturbation series.